CHEMISTRY
A EUROPEAN JOURNAL

DOI: 10.1002/chem.200701750

Oxidative Homolysis of a Nitrosylchromium Complex

Wenjing Song and Andreja Bakac*[a]

Abstract: Metal(III)–polypyridine complexes $[M(NN)_3]^{3+}$ (M = Ru or Fe; NN = bipyridine (bpy), phenanthroline (phen), or 4,7-dimethylphenanthroline (Me_2-phen)) oxidize the nitrosylpentaaquachromium(III) ion, $[Cr_{aq}NO]^{2+}$, with an overall 4:1 stoichiometry, $4[Ru(bpy)_3]^{3+} + [Cr_{aq}NO]^{2+} + 2H_2O \rightarrow 4[Ru(bpy)_3]^{2+} + [Cr_{aq}]^{3+} + NO_3^- + 4H^+$. The kinetics follow a mixed second-order rate law, $-d[[M(NN)_3]^{3+}]/dt = nk[[M(NN)_3]^{3+}][[Cr_{aq}NO]^{2+}]$, in which k represents the rate constant for the initial one-electron transfer step, and $n = 2$–4 depending on reaction conditions and relative rates of the first and subsequent steps. With $[Cr_{aq}NO]^{2+}$ in excess, the values of nk are 283 $M^{-1}s^{-1}$ ($[Ru(bpy)_3]^{3+}$), 7.4 ($[Ru(Me_2\text{-phen})_3]^{3+}$), and 5.8 ($[Fe(phen)_3]^{3+}$). In the proposed mechanism, the one-electron oxidation of $[Cr_{aq}NO]^{2+}$ releases NO, which is further oxidized to nitrite, $k = 1.04\times10^6\ M^{-1}s^{-1}$, 6.17×10^4, and 1.12×10^4 with the three respective oxidants. Further oxidation yields the observed nitrate. The kinetics of the first step show a strong correlation with thermodynamic driving force. Parallels were drawn with oxidative homolysis of a superoxochromium(III) ion, $[Cr_{aq}OO]^{2+}$, to gain insight into relative oxidizability of coordinated NO and O_2, and to address the question of the "oxidation state" of coordinated NO in $[Cr_{aq}NO]^{2+}$.

Keywords: chromium · homolysis · kinetics · nitric oxide · oxidation

Introduction

Nitric oxide is recognized as an essential agent in a number of physiological processes that play a role in blood pressure regulation, neurotransmission, and immune response.[1–6] Understanding the mechanism of action of NO in vivo, and the design of NO delivery compounds[7–9] as drugs for the treatment of NO-imbalance diseases requires detailed knowledge of mechanistic chemistry of NO and NO-containing compounds. As a result, a large number of insightful mechanistic studies of the binding and release of NO by transition-metal complexes and other substances have been carried out.[3,10–12] Among metal complexes, iron–porphyrins have received most attention,[11,13,14] but non-porphyrin complexes of a number of metal ions have also provided important mechanistic data on the formation and chemistry of metal nitrosyls.[10,12,15–17]

Thermal and photochemical cleavage of a metal–NO bond, and the low pH-induced dissociation of NO from NONOates are among the most common ways of generating NO for chemical and biological purposes. Several other mechanisms for NO release exist, and it is quite likely that some of them may be advantageous under some circumstances. One possibility is oxidative homolysis, that is, oxidation induced release of NO from a metal nitrosyl. Recently, Herold and co-workers discovered that the oxidation of nitrosyl hemes with peroxynitrite[18] and with nitrogen dioxide[19] at a neutral pH generates Fe^{III} hemes and NO. This chemistry is consistent with the greater lability of Fe^{III}–NO than of Fe^{II}–NO, a pattern that has been established in earlier studies.

To the best of our knowledge, only non-metallic oxidants have been observed so far to induce oxidative homolysis of nitrosyl complexes. In search of metal-induced oxidative homolysis, and some insight into the relevance of such a mechanism in chemical and biological environments, we have now examined the reaction between metal–polypyridine oxidants and a chromium nitrosyl ion, $[Cr_{aq}NO]^{2+}$.

The metal nitrosyl that we chose for this study has been known for several decades, although its precise electronic structure has never been completely established. Arguments for both $Cr^I(NO^+)$ and $Cr^{III}(NO^-)$ forms have been advanced. The NO stretch of 1747 cm^{-1}, magnetic moment of 2.2 μ_B, and the EPR spectrum[20] appear consistent with the $Cr^I(NO^+)$ form.[21] The crystal structure,[22] low substitution

[a] Dr. W. Song, Prof. A. Bakac
Iowa State University, Ames, IA 50011 (USA)
Fax: (+1) 515-294-5233
E-mail: bakac@iastate.edu

Supporting information for this article is available on the WWW under http://www.chemeurj.org/ or from the author.

rates, a pK_a of 4.8,[23] pronounced *trans*-labilization by coordinated NO,[21] and, most convincingly, the XAS spectrum[24] are, on the other hand, diagnostic of the $Cr^{III}(NO^-)$ form. Ab initio calculations[25] support a 2+ charge on the chromium. Clearly, all the limiting forms are only approximations, and none represents a completely accurate picture. We reasoned that electron-transfer reactions should provide an additional angle that would shed more light on the issue of electronic structure.

In particular, a comparison between superoxo and nitrosyl complexes should be informative in both kinetic and mechanistic sense. The complex $[Cr_{aq}OO]^{2+}$ has been characterized spectroscopically and chemically.[26–28] All the data strongly support the Cr^{III}–superoxide description, as opposed to Cr^{II}–O_2 or Cr^{IV}–peroxide. We have previously studied the oxidation of $[Cr_{aq}OO]^{2+}$ by metal polypyridine complexes of ruthenium and iron,[29] and will now use these data as a baseline against which the redox behavior of $[Cr_{aq}NO]^{2+}$ will be gauged. It is advantageous for our purpose that the ligand system is identical in the nitrosyl and superoxo complexes.

Results

$[Ru(bpy)_3]^{3+}$ as oxidant: Freshly prepared photogenerated $[Ru(bpy)_3]^{3+}$ reacted rapidly with $[Cr_{aq}NO]^{2+}$ in acidic aqueous solution. The high acid concentration (typically 1.0 M) was necessary to slow the spontaneous reduction of $[Ru(bpy)_3]^{3+}$. From the absorbance increase at 452 nm, at which the product $[Ru(bpy)_3]^{2+}$ exhibits a maximum ($\varepsilon = 1.45\times10^4\,M^{-1}\,cm^{-1}$), the stoichiometric ratio $\Delta[[Ru(bpy)_3]^{3+}]/\Delta[[Cr_{aq}NO]^{2+}]$ was determined to be 3.8, close to the expected ratio of 4.0, Figure S1 in the Supporting Information and Equation (1).

$$4[Ru(bpy)_3]^{3+}+[Cr_{aq}NO]^{2+}+2\,H_2O \rightarrow 4\,[Ru(bpy)_3]^{2+}+ [Cr_{aq}]^{3+}+NO_3^-+4\,H^+ \quad (1)$$

Kinetic traces obtained at 452 nm with $[Cr_{aq}NO]^{2+}$ in large excess were fitted to a single-exponential rate law, and yielded pseudo-first-order rate constants k_{obs}. A plot of k_{obs} against the concentration of $[Cr_{aq}NO]^{2+}$ is linear with a slope $k_{CrNO} = (283\pm2)\,M^{-1}s^{-1}$ in 1.0 M $HClO_4$. A series of kinetic runs in 0.24 M $HClO_4$ behaved similarly, and yielded $k_{CrNO} = (405\pm18)\,M^{-1}s^{-1}$ (see Figure S2 in the Supporting Information) showing that the reaction exhibits only a mild dependence on acid concentration and/or ionic strength. Experiments with excess $[Ru(bpy)_3]^{3+}$ were attempted, but the results proved unreliable because the loss of the oxidant to background decomposition became quite serious under such conditions.

A number of considerations, but most notably the 4:1 stoichiometry of Equation (1), suggest that a series of steps and intermediates, such as NO and HNO_2/NO_2^-, are involved in the $[Cr_{aq}NO]^{2+}/[Ru(bpy)_3]^{3+}$ reaction. We decided to examine directly the potential individual steps to get a better insight and understanding of the overall mechanism, as described in the following sections.

The reaction between NO and excess $[Ru(bpy)_3]^{3+}$ was found to be too fast to measure by conventional spectrophotometric methods at several micromolar concentrations of each reagent. Only a jump in absorbance at 452 nm could be observed upon mixing of the two reactants. The size of the absorbance jump was linearly related to the concentration of added NO, and yielded a 1:1 $[Ru(bpy)_3]^{3+}$/NO stoichiometry. This step was followed by a slower absorbance increase, Figure 1.

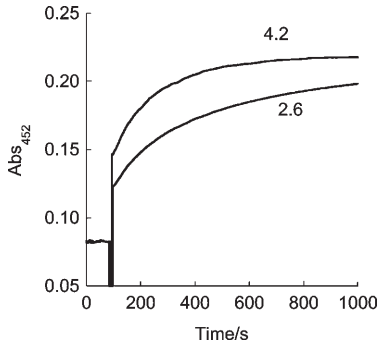

Figure 1. Kinetic traces obtained upon mixing of 10 μM $[Ru(bpy)_3]^{3+}$ with NO (4.2 μM, top, 2.6 μM, bottom) in 1.0 M $HClO_4$.

The kinetics of the first, fast step in the $[Ru(bpy)_3]^{3+}$/NO reaction (jump in Figure 1) were determined with a stopped-flow apparatus with NO in large excess over $[Ru(bpy)_3]^{3+}$. The kinetic traces were exponential, and a plot of k_{obs} against [NO] was linear (Figure S3 in the Supporting Information), yielding $k_{NO} = (1.04\pm0.02)\times10^6\,M^{-1}s^{-1}$.

The rate constant for the slower step in Figure 1 was calculated from the initial rates by assuming first-order dependence on $[Ru(bpy)_3]^{3+}$ and on the product of NO oxidation in the first step, believed to be nitrite ion. The value obtained, $(1200\pm50)\,M^{-1}s^{-1}$, is similar to, although somewhat smaller than that determined independently for the $[Ru(bpy)_3]^{3+}$/nitrite reaction in 1.0 M $HClO_4$, $k = 1740\,M^{-1}s^{-1}$; see later. The rather large deviation can be explained by the uncertainty in concentrations at the zero time for the second step in Figure 1. The results suggest the sequence of events described by Equations (2)–(4).

$$[Ru(bpy)_3]^{3+}+NO \xrightarrow{k_2} [Ru(bpy)_3]^{2+}+NO^+ \quad (2)$$

$$NO^+ + H_2O \underset{k_{-3}}{\overset{k_3}{\rightleftharpoons}} HNO_2 + H^+ \quad \text{fast} \quad (3)$$

$$[Ru(bpy)_3]^{3+}+HNO_2/NO_2^- \overset{k_4}{\rightleftharpoons} [Ru(bpy)_3]^{2+}+NO_2 \quad (4)$$

The $[Ru(bpy)_3]^{3+}$/nitrite reaction was studied with nitrite in pseudo-first-order excess. At a constant acid concentration, the reaction obeyed a mixed second-order rate law, as illustrated by excellent fits to the exponential rate equation

and linear dependence of k_{obs} so obtained against $[NO_2^-]$ (Figure S4 in the Supporting Information). The $[H^+]$ dependence of the second-order rate constant is depicted in Figure 2 as a plot of k versus $[H^+]^{-1}$. The plot is linear with

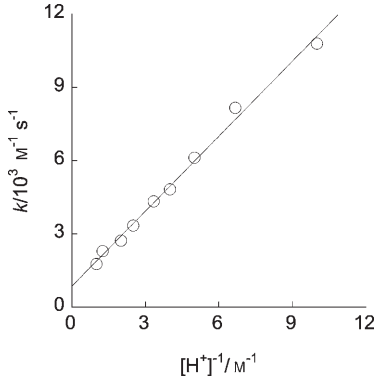

Figure 2. Plot of second-order-rate constant for the $[Ru(bpy)_3]^{3+}$/nitrite reaction against reciprocal acid concentration at 1.0 M ionic strength. $[NO_2^-]=40$–$500\ \mu M$, $[[Ru(bpy)_3]^{3+}]=2$–$10\ \mu M$.

a slope $k_{-1}=(1.02\pm0.03)\times10^3\ s^{-1}$ and an intercept $k_0=(0.86\pm0.15)\times10^3\ M^{-1}s^{-1}$. The complete rate law is thus given by Equation (5), in which $[NO_2^-]_{tot}=\{[NO_2^-]+[HNO_2]\}$. The two forms are related by an acidity constant $K_a=6.3\times10^{-4}$ [Eq. (6)].[30]

$$\frac{-d[[Ru(bpy)_3]^{3+}]}{dt}=(k_0+k_{-1}[H^+]^{-1})[[Ru(bpy)_3]^{3+}][NO_2^-]_{tot} \quad (5)$$

$$HNO_2 \rightleftharpoons H^+ + NO_2^- \quad K_a \quad (6)$$

The straightforward interpretation of the two-term rate law associates the k_{-1} term with the reaction of NO_2^-, and the k_0 term with HNO_2. The complete rate law for such a case is given in Equation (7), which reduces to the observed form in the limit $K_a \ll [H^+]$. The parameter k_{-1} in Equation (5) is now identified as the product $K_a k'_{-1}$, in which $k'_{-1}=1.62\times10^6\ M^{-1}s^{-1}$ represents the specific rate constant for the reaction of the anion NO_2^- with $[Ru(bpy)_3]^{3+}$.

$$\text{Rate}=\frac{k_0[H^+]+k'_{-1}K_a}{K_a+[H^+]}[[Ru(bpy)_3]^{3+}][NO_2^-]_{tot} \quad (7)$$

The rate law in Equation (7) identifies k_0 as a bimolecular rate constant for the $HNO_2/[Ru(bpy)_3]^{3+}$ reaction, although we cannot rule out the possibility that HNO_2 reduces $[Ru(bpy)_3]^{3+}$ by disproportionation,[31] Equation (8), followed by the $[Ru(bpy)_3]^{3+}$/NO reaction of Equation (2). From the available rate constants for the reactions given in Equations (2) and (8),[31] we estimate that Equation (8), which is catalyzed by H^+,[31] contributes only about 25% of the acid-independent term at 1.0 M H^+, and significantly less at lower $[H^+]$ in Figure 2. The direct $[Ru(bpy)_3]^{3+}/HNO_2$ reaction thus appears responsible for the major portion of the k_0 term. The observed first-order dependence on $[HNO_2]$ and good fits to exponential rate law when $[HNO_2] \gg [Ru(bpy)_3^{3+}]$ also require that the contribution from a second-order term of Equation (8) be minor.

$$2\,HNO_2 \rightleftharpoons NO + NO_2 + H_2O \quad (8)$$

$[Fe(phen)_3]^{3+}$ as oxidant: The reaction with $[Cr_{aq}NO]^{2+}$ was much slower than the $[Ru(bpy)_3]^{3+}/[Cr_{aq}NO]^{2+}$ reaction. The rate constant was evaluated from initial rates using 3–5 μM $[Fe(phen)_3]^{3+}$ and 0.10–0.40 mM $[Cr_{aq}NO]^{2+}$ in 0.10 M $HClO_4$, as illustrated in Figure S5 in the Supporting Information. It was necessary to use lower ionic strength (and, thus, lower acid concentration) to prevent the Fe^{II} product from precipitating. We presume that the $[H^+]$ effect on the kinetics is minor, similar to that established in the $[Ru(bpy)_3]^{3+}$ reaction. The data at 0.10 M H^+ yielded the rate constant $k=(5.8\pm0.4)\ M^{-1}\ s^{-1}$.

The kinetics of the reaction of $[Fe(phen)_3]^{3+}$ with NO (0.050–0.30 mM) were determined by stopped flow measurements, $k=(1.12\pm0.05)\times10^4\ M^{-1}s^{-1}$ in 0.10 M $HClO_4$, Figure S6 in the Supporting Information.

The oxidation of nitrite with $[Fe(phen)_3]^{3+}$ in 0.10 M $HClO_4$ generated kinetic traces that could be fitted to a single exponential only when the concentration of nitrite (0.2–1.2 mM) was in excess and much larger than required to satisfy pseudo-first-order conditions at the typical concentrations of $[Fe(phen)_3]^{3+}$ of $\leq 10\ \mu M$. A plot of pseudo-first-order rate constants obtained under such conditions against the concentration of nitrite was linear and yielded a second-order rate constant of $(3.24\pm0.05)\times10^3\ M^{-1}s^{-1}$ in 0.10 M $HClO_4$. Assuming that nitrite anion is the exclusive reactive form at this $[H^+]$, then the specific rate constant for the $NO_2^-/[Fe(phen)_3]^{3+}$ reaction is calculated to be $5.14\times10^5\ M^{-1}s^{-1}$. At smaller excesses of nitrite, the apparent rate constant decreased with time during the course of the reaction in a manner that suggested inhibition by reaction products, as shown in Figure S7 in the Supporting Information. Indeed, adding external $[Fe(phen)_3]^{2+}$ to reaction solutions had a strong retarding effect. A series of experiments was carried out with 5–10 μM $[Fe(phen)_3]^{3+}$, 37 μM NO_2^-, and 0–80 μM added $[Fe(phen)_3]^{2+}$ in 0.10 M CF_3SO_3H. (In these experiments, CF_3SO_3H replaced $HClO_4$ because the latter caused the iron(II) complex to precipitate at these high concentrations.) The first 50 s of each trace was fitted to the first-order rate law. The approximate pseudo-first-order rate constants so obtained were divided by the total nitrite concentration and plotted against the average $[[Fe(phen)_3]^{2+}]$ in Figure 3, which clearly illustrates the inhibiting effect of $[Fe(phen)_3]^{2+}$.

The effect of $[Fe(phen)_3]^{2+}$ is easily understood in light of the reduction potentials of the two couples, $NO_2^{\cdot}/NO_2^-$ (1.04 V versus NHE)[32] and $[Fe(phen)_3]^{3+/2+}$ (1.06 V).[33] At 0.10 M H^+ used in this work, and taking K_a for HNO_2 as 6.3×10^{-4} M,[30] the equilibrium constant for the reaction given in Equation (9) is 0.014. The accumulation of [Fe-

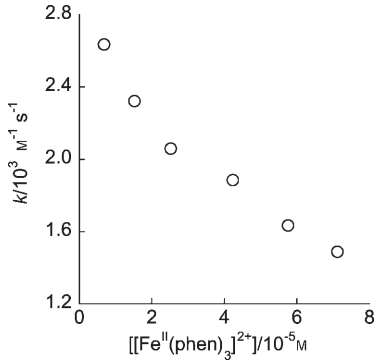

Figure 3. Plot of second-order-rate constants for the $[Fe(phen)_3]^{3+}$/nitrite reaction at different concentrations of added $[Fe(phen)_3]^{2+}$ in 0.10 M CF_3SO_3H. $[[Fe(phen)_3]^{3+}] = 5$–10 μM, $[NO_2^-]_{tot} = 37$ μM.

$(phen)_3]^{2+}$ and its inhibiting effect increase with the progress of the reaction, but the effect reveals itself only in the kinetics. The final product yields are always quantitative because one of the products, $NO_2^{\cdot}$, undergoes irreversible dimerization/disproportionation and pulls the overall reaction to completion, Equation (10). Similar retarding effect of the iron(II) product was observed in the reduction of $[Fe(3,4,7,8\text{-}Me_4\text{-}phen)_3]^{3+}$ by nitrite.[34]

$$[Fe(phen)_3]^{3+} + NO_2^- \rightleftharpoons [Fe(phen)_3]^{2+} + NO_2 \quad (9)$$

$$2\,NO_2 \underset{k_{-10}}{\overset{k_{10}}{\rightleftharpoons}} N_2O_4 \xrightarrow{H_2O,\ k_{10a}} NO_3^- + HNO_2 + H^+ \quad (10)$$

The behavior of the complex $[Ru(Me_2\text{-}phen)_3]^{3+}$ in its reactions with $[Cr_{aq}NO]^{2+}$, NO, and nitrite under the conditions of limited $[Ru(Me_2\text{-}phen)_3]^{3+}$ was similar to that of the other two oxidants. From the initial rates, Table S1 in the Supporting Information, the overall rate constant $k = (7.4 \pm 0.9)$ M^{-1} s^{-1} was obtained for the reaction with $[Cr_{aq}NO]^{2+}$. The plots of the pseudo-first-order rate constants for the reactions with NO and with nitrite are shown in Figure S8 and S9, respectively, in the Supporting Information. All the rate constants obtained in this work are summarized in Table 1. Data for the NO reactions with $[Fe(phen)_3]^{3+}$ and $[Ru(Me_2\text{-}phen)_3]^{3+}$ in Table 1 were corrected for the contribution from the nitrite reaction with the same oxidants. Nitrite is present at about 0.2 mM level in our stock solutions of NO. In no case was the correction greater than 4% of the experimentally measured value.

Table 1. Kinetic data for oxidation of $[Cr_{aq}NO]^{2+}$, NO and NO_2^- by $[M(NN)_3]^{3+}$.

	nk [M^{-1} s^{-1}][a] $[Cr_{aq}NO]^{2+}$	k [10^6 M^{-1} s^{-1}] NO	k [10^6 M^{-1} s^{-1}] NO_2^-	$[H^+]$ [M]
$[Ru(bpy)_3]^{3+}$	283	1.04	1.62[b]	1.00
$[Ru(Me_2\text{-}phen)_3]^{3+}$	7.4	0.0617	1.63	0.10
$[Fe(phen)_3]^{3+}$	5.8	0.0112	0.514	0.10

[a] Experimental value, not corrected for stoichiometric factor n, see text. [b] The reaction also exhibits an acid independent term corresponding to HNO_2 reaction, $k = 860$ M^{-1} s^{-1}.

Discussion

$[Cr_{aq}NO]^{2+}$ is inert toward ordinary oxidants such as molecular oxygen or hydrogen peroxide, but it can be oxidized by the powerful two-electron oxidants[23] BrO_3^- and IO_4^-. An inner-sphere mechanism was proposed in both cases.[23]

The present study shows that $[Cr_{aq}NO]^{2+}$ also reacts with metallic outer-sphere oxidants. All the data obtained in this work point to a reaction sequence beginning with the rate-determining one-electron oxidation of $[Cr_{aq}NO]^{2+}$ followed by a series of steps that ultimately generate $[Cr_{aq}]^{3+}$ and nitrate, as shown for the $[Ru(bpy)_3]^{3+}$ [Eqs. (2)–(4) and (10) and (11)].

$$[Ru(bpy)_3]^{3+} + [Cr_{aq}NO]^{2+} \xrightarrow{k_{11}} [Ru(bpy)_3]^{2+} + [Cr_{aq}]^{3+} + NO \quad (11)$$

The support for this mechanism comes from the observed 4:1 stoichiometry and independent, direct observation of all the individual steps given in Equations (2)–(4) and (10) and (11). Reactions (11), (2), and (4) were studied in this work, and detailed information for the remaining steps (3)[35,36] and (10)[36] exists in the literature. With all the necessary data at hand, we utilized the program Kinsim to simulate kinetic traces under our experimental conditions. The agreement with observed traces is excellent for experiments using excess $[Cr_{aq}NO]^{2+}$. Only minor deviations, believed to be caused by less than perfect correction for the slow background decay of $[Ru(bpy)_3]^{3+}$, are seen in the trace obtained with excess $[Ru(bpy)_3]^{3+}$, Figure 4. The good agreement between the experiment and simulation provides additional credibility for the proposed mechanism.

The first step, reaction 11, is written as a single stage process that generates Cr_{aq}^{3+} and NO as separate species. It is quite likely that an unstable $Cr_{aq}NO^{3+}$ intermediate is formed first, followed by dissociation of NO, similar to the oxidation of $MbFe^{II}NO$ with NO_2 and $HOONO/OONO^-$ which yielded the intact $MbFe^{III}NO$ prior to NO release. We have no evidence for the involvement of $Cr_{aq}NO^{3+}$ in reaction 11. If formed, this intermediate must be short-lived, given that the step following reaction 11 is fast, see below. Intermediates generated by oxidation of other $Cr_{aq}X^{2+}$ complexes ($X = O_2$ or alkyl)[29,37] and of $CpCr^{II}(NO)Cl_2^-$[38] are also too short-lived to be observed.

The 4:1 $[Ru(bpy)_3]^+/[Cr_{aq}NO]^{2+}$ stoichiometry was determined under conditions of excess $[Ru(bpy)_3]^{3+}$. Most of the kinetic experiments with all three oxidants, on the other hand, used excess $[Cr_{aq}NO]^{2+}$, a condition that will, under some circumstances, reduce the overall stoichiometry and affect the kinetics as well. The rate constants listed in the second column in Table 1 represent the product nk_{11}, in which n is the stoichiometric factor applicable under the conditions of the experiment [Eq. (12)].

$$\frac{-d[[M(NN)_3]^{3+}]}{dt} = nk_{11}[[Cr_{aq}NO]^{2+}][[M(NN)_3]^{3+}] \quad (12)$$

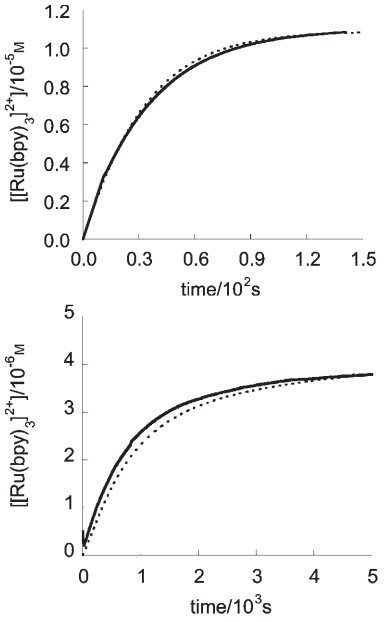

Figure 4. Experimental (solid) and simulated (dashed) kinetic traces for the reaction of 11 μM $[Ru(bpy)_3]^{3+}$ with 100 μM $[Cr_{aq}NO]^{2+}$ (top) and 0.8 μM $[Cr_{aq}NO]^{2+}$ (bottom) in 1.0 M $HClO_4$. Simulations according to the mechanism in depicted in Scheme 1 utilized the following rate constants (obtained in this work and ref. [31]): $k_{11}=142\,M^{-1}s^{-1}$, $k_2=1.0\times10^6\,M^{-1}\,s^{-1}$, $k_4=1.88\times10^3\,M^{-1}s^{-1}$, $k_{10}=5\times10^8\,M^{-1}s^{-1}$, $k_{-10}=7\times10^3\,s^{-1}$, $k_{10a}=1\times10^3\,s^{-1}$, K_a for $HNO_2=6.3\times10^{-4}$ M, and k_{decay} (for background decay of $[Ru(bpy)_3]^{3+}$) $=1.6\times10^{-5}\,s^{-1}$.

Table 2. Results of kinetic simulations for reactions of $[Cr_{aq}NO]^{2+}$ with $[M(NN)_3]^{3+}$.

	k_{11} [$M^{-1}s^{-1}$][a]	n[b]	k_{CrOO} [$M^{-1}s^{-1}$][c]
$[Ru(bpy)_3]^{3+}$	142	2	2630
$[Ru(Me_2\text{-}phen)_3]^{3+}$	3.7	2	1060
$[Fe(phen)_3]^{3+}$	1.4	4	82

[a] Obtained from simulations according to the mechanism in Scheme 1, see text. [b] Stoichiometric factor under the experimental conditions. [c] Rate constant for the oxidation of $[Cr_{aq}OO]^{2+}$. Data from reference [29].

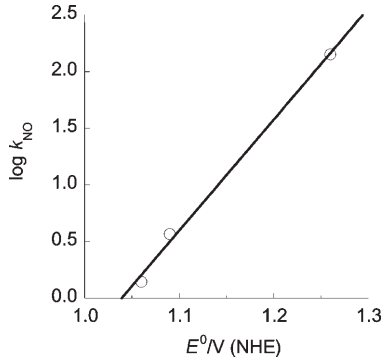

Figure 5. Plot of $\log k_{11}$ ($=\log k_{NO}$) for the reaction between $[Ru(bpy)_3]^{3+}$ and $[Cr_{aq}NO]^{2+}$ versus reduction potential of $[Ru(bpy)_3]^{3+}$, $[Ru(Me_2\text{-}phen)_3]^{3+}$, and $[Fe(phen)_3]^{3+}$.

The data in Table 1 show that the oxidant/NO reaction is always fast relative to the initial step [Eq. (11) and analogues] under our experimental conditions, that is, with concentrations of $[Cr_{aq}NO]^{2+}\leq0.4$ mM and $[Ru(bpy)_3]^{3+}\approx0.01$ mM, but that the next step, oxidation of nitrite, may not be "fast" at the high H^+ concentrations used in this work. Similarly, reagent concentrations and individual rate constants for various steps in Equations (2)–(4) and (10) and (11) will determine the steady-state concentrations of NO_2 and thus the rate of reaction (10) relative to reaction (11) and the reverse of reaction (4). The values of n were estimated by calculating the pseudo rate constants for each step from the known rate constants and experimental concentrations, and determining whether these rates are "slow" or "fast" relative to the experimental value for the overall reaction. The major reason for the variation in n among the three complexes are the different ratios k_{11}/k_4, and the use of higher $[H^+]$ (1.0 M) in the $[Cr_{aq}NO]^{2+}/[Ru(bpy)_3]^{3+}$ reaction than in the reactions of the other two oxidants (0.10 M).

Also shown in Table 2 are the data for the oxidation of $[Cr_{aq}OO]^{2+}$ by the same three oxidants. In that reaction, the stoichiometric factor n is always 1.0.[29]

There is a strong correlation between the rate constants k_{11} and the thermodynamic driving force for the reaction. The plot of $\log k_{11}$ (denoted in Figure 5 as k_{NO}) against the reduction potential of the oxidant is linear with a slope of 9.5, reasonably close to the value of 8.4 expected on the basis of Marcus theory. This result is consistent with an outer-sphere mechanism, which is favored in view of the substitutional inertness and lack of feasible coordination site on the $[M(NN)_3]^{3+}$ oxidants.

A correlation similar to that in Figure 5 is obtained for the oxidation of $[Cr_{aq}OO]^{2+}$ by the same three oxidants,[29] although the scatter of the data is somewhat greater for the superoxo complex. As shown in Table 2, the kinetics of oxidation of $[Cr_{aq}NO]^{2+}$ and $[Cr_{aq}OO]^{2+}$ are quite similar, with the two series lying within two orders of magnitude from each other.

The reduction potentials for the free couples are −0.16 V (O_2/O_2^-, standard state 1 M)[39] and −(0.8±0.2) V ($NO/^3NO^-$).[40] The calculation of the reduction potentials for dissociative oxidation of the chromium complexes, E^0_{dissoc}, of these (anionic) ligands also requires the knowledge of the equilibrium binding constants K_{Cr}, as shown in Scheme 1.

$$NO + e^- \rightleftharpoons NO^- \qquad E^0$$
$$NO^- + [Cr_{aq}]^{3+} \rightleftharpoons [Cr_{aq}NO]^{2+} \qquad K_{Cr}$$
$$\text{Net: } NO + [Cr_{aq}]^{3+} + e^- \rightleftharpoons [Cr_{aq}NO]^{2+} \qquad E^0_{dissoc}$$

Scheme 1.

Unfortunately, the value of K_{Cr} for $[Cr_{aq}NO]^{2+}$ is not known, but it has to be much greater than K_{Cr} for $[Cr_{aq}OO]^{2+}$ ($3\times10^8\,M^{-1}$, calculated from the equilibrium constant for $[Cr_{aq}]^{2+}$–O_2 bond homolysis and reduction poten-

tials for $[Cr_{aq}]^{3+/2+}$ and O_2/O_2^-). The idea of the stronger binding of NO^- than of O_2^- to the metal is also supported by the much stronger binding of the proton to NO^-, $pK_a = 11.4$ for $^1HNO/^3NO^-$)[41] and 4.7 for HO_2/O_2^-.[42] On these grounds we conclude that the gap between the potentials for the two complexes should be much smaller than that for the free anions, as is the case with the two conjugate acids ($E^0 = 0.16$ V for O_2/HO_2[39] and -0.14 for $^3NO/^1HNO$).[41] Thus the lower reactivity of $[Cr_{aq}NO]^{2+}$ is most likely the result of the changed thermodynamics of the coordinated versus free anions.

To support our argument, we searched the literature for other examples of oxidation of superoxo and nitrosyl complexes with transition-metal oxidants. Unfortunately, the data are quite limited, and the only related examples appear to be the reactions of oxy[43] and nitrosyl[18] hemoglobins and myoglobins with peroxynitrite. The oxidation of the nitrosyl complexes is a one-electron reaction, but the oxy species are oxidized to Fe^{IV} in a two-electron process. At a given pH, the rate constants for the nitrosyl and oxy globins are quite similar, but the meaning of this finding is dubious in view of the mechanistic differences.

Based on our analysis, and in view of the observed similarity with the superoxo complex in the reactions with oxidants, we conclude that the Cr^{III}–NO^- form provides the best description of the nitrosyl complex. Just as in the case of $[Cr_{aq}{}^{III}OO]^{2+}$ and other superoxo complexes,[44–46] this limiting form is clearly an oversimplification, but one that is none the less quite useful in rationalizing the observed chemistry.

Experimental Section

Solutions of $[Cr_{aq}NO]^{2+}$ were prepared from $[Cr_{aq}]^{2+}$ and NO by a literature procedure,[47] and purified by ion exchange on Sephadex C-25. The concentration of $[Cr_{aq}NO]^{2+}$ was determined spectrophotometrically (λ_{max} 449 nm, $\varepsilon = 121\ M^{-1}cm^{-1}$).[47] Gaseous NO (Matheson) was purified by passage through Ascarite, sodium hydroxide and water.[48] Stock solutions of NO were prepared by bubbling the purified gas through argon-saturated 0.10 M or 1.0 M $HClO_4$ for 30 min.[48] Such solution typically contained 1.7 mM NO and 0.2 mM nitrite ions. Solutions of $[Cr_{aq}]^{2+}$ were generated by zinc amalgam reduction of $[Cr_{aq}]^{3+}$. The complex salts $[Fe(phen)_3][ClO_4]_3$[49] and $[Ru(Me_2\text{-}phen)_3]Cl_2{\cdot}6H_2O$[50] were prepared by literature procedures. $[Ru(bpy)_3]Cl_2$, $Cr[ClO_4]_3{\cdot}6H_2O$, and trifluoromethanesulfonic acid were purchased from Aldrich. $HClO_4$ (70%) and sodium nitrite (99.999%) were from Fisher Scientific.

Solutions of $[Ru(bpy)_3]^{3+}$ and $[Ru(Me_2\text{-}phen)_3]^{3+}$ were generated photochemically from the corresponding 2+ ions and an excess of $[Co(NH_3)_5(H_2O)]^{3+}$ (2 mM) by exposing the sample to Pyrex-filtered sunlight.[51] The kinetic experiments typically utilized small concentrations (1–10 μM) of the metal–polypyridine complexes and a large excess of the reductant (metal nitrosyl complexes, NO, or nitrite). Ionic strength was adjusted with $HClO_4$ and $LiClO_4$.

Kinetic and UV/Vis spectral measurements were made with a Shimadzu 3101 PC spectrophotometer at 25.0 ± 0.1 °C. For fast reactions, an Applied Photophysics stopped-flow spectrophotometer was used. Kinetic analyses were performed with KaleidaGraph 3.6 PC software. Simulations were performed with the Kinsim/Fitsim[52] software for PC.

Acknowledgement

This work was supported by a grant from National Science Foundation, CHE 0602183. Some of the work was conducted with the use of facilities at the Ames Laboratory.

[1] R. M. J. Palmer, A. G. Ferrige, S. Moncada, *Nature* **1987**, *327*, 524–526.
[2] T. W. Hayton, P. Legzdins, W. B. Sharp, *Chem. Rev.* **2002**, *102*, 935–991.
[3] P. C. Ford, I. M. Lorkovic, *Chem. Rev.* **2002**, *102*, 993–1017.
[4] B. A. Averill, *Chem. Rev.* **1996**, *96*, 2951–2964.
[5] S. Moncada, R. M. J. Palmer, E. A. Higgs, *Pharmacol. Rev.* **1991**, *43*, 109–142.
[6] *Nitric Oxide. Biology and Pathobiology* (Ed.: L. J. Ignarro), Academic Press, San Diego, **2000**.
[7] J. H. Shin, S. K. Metzger, M. H. Schoenfisch, *J. Am. Chem. Soc.* **2007**, *129*, 4612–4619.
[8] A. A. Eroy-Reveles, Y. Leung, P. K. Mascharak, *J. Am. Chem. Soc.* **2006**, *128*, 7166–7167.
[9] M. J. Clarke, *Coord. Chem. Rev.* **2003**, *236*, 209–233.
[10] P. C. Ford, L. E. Laverman, *Coord. Chem. Rev.* **2005**, *249*, 391–403.
[11] I. M. Wasser, S. de Vries, P. Moeenne-Locoz, I. Schroeder, K. D. Karlin, *Chem. Rev.* **2002**, *102*, 1201–1234.
[12] M. Wolak, R. van Eldik, *Coord. Chem. Rev.* **2002**, *230*, 263–282.
[13] A. Ghosh, *Acc. Chem. Res.* **2005**, *38*, 943–954.
[14] A. J. Gow, A. P. Payson, J. Bonaventura, *J. Inorg. Biochem.* **2005**, *99*, 903–911.
[15] F. Roncaroli, M. Videla, L. D. Slep, J. A. Olabe, *Coord. Chem. Rev.* **2007**, *251*, 1903–1930.
[16] A. Nemes, O. Pestovsky, A. Bakac, *J. Am. Chem. Soc.* **2002**, *124*, 421–427.
[17] O. Pestovsky, A. Bakac, *J. Am. Chem. Soc.* **2002**, *124*, 1698–1703.
[18] S. Herold, F. Boccini, *Inorg. Chem.* **2006**, *45*, 6933–6943.
[19] F. Boccini, A. S. Domazou, S. Herold, *J. Phys. Chem. A* **2006**, *110*, 3927–3932.
[20] P. H. Rieger, *Coord. Chem. Rev.* **1994**, *135/136*, 203–286.
[21] M. Ardon, S. Cohen, *Inorg. Chem.* **1993**, *32*, 3241–3243.
[22] M. Ardon, S. Cohen, *Inorg. Chem.* **1993**, *32*, 3241–3243.
[23] A. K. Jhanji, E. S. Gould, *Inorg. Chem.* **1990**, *29*, 3890–3892.
[24] A. Levina, P. Turner, P. A. Lay, *Inorg. Chem.* **2003**, *42*, 5392–5398.
[25] I. Shim, K. A. Gingerich, K. Mandix, X. Feng, *Inorg. Chim. Acta* **1995**, *229*, 455–460.
[26] A. Bakac, *Prog. Inorg. Chem.* **1995**, *43*, 267–351.
[27] A. Bakac, *Adv. Inorg. Chem.* **2004**, *55*, 1–59.
[28] A. Bakac, *Coord. Chem. Rev.* **2006**, *250*, 2046–2058.
[29] A. Bakac, J. H. Espenson, J. A. Janni, *J. Chem. Soc. Chem. Commun.* **1994**, 315.
[30] N. N. Greenwood, A. Earnshaw, *Chemistry of the Elements*, 2nd ed., **1997**.
[31] O. Pestovsky, A. Bakac, *Inorg. Chem.* **2002**, *41*, 901–905.
[32] D. M. Stanbury, *Adv. Inorg. Chem.* **1989**, *33*, 69–138.
[33] N. Sutin, C. Creutz, *Adv. Chem. Ser.* **1978**, *168*, 1–27.
[34] M. S. Ram, D. M. Stanbury, *J. Am. Chem. Soc.* **1984**, *106*, 8136–8142.
[35] N. S. Bayliss, R. Dingle, D. W. Watts, R. J. Wilkie, *Aust. J. Chem.* **1963**, *16*, 933–942.
[36] G. Stedman, *Adv. Inorg. Chem. Radiochem.* **1979**, *22*, 113–170.
[37] J. D. Melton, A. Bakac, J. H. Espenson, *Inorg. Chem.* **1986**, *25*, 4104–4108.
[38] P. Legzdins, W. S. McNeil, S. J. Rettig, K. M. Smith, *J. Am. Chem. Soc.* **1997**, *119*, 3513–3522.
[39] D. T. Sawyer, in *Oxygen Complexes and Oxygen Activation by Transition Metals* (Eds.: A. E. Martell, D. T. Sawyer), Plenum, New York, **1988**.
[40] M. D. Bartberger, W. Liu, E. Ford, K. M. Miranda, C. Switzer, J. M. Fukuto, P. J. Farmer, D. A. Wink, K. N. Houk, *Proc. Natl. Acad. Sci. USA* **2002**, *99*, 10958–10963.

[41] V. Shafirovich, S. V. Lymar, *Proc. Natl. Acad. Sci. USA* **2002**, *99*, 7340–7345.
[42] B. H. Bielski, *Photochem. Photobiol.* **1978**, *28*, 645–649.
[43] F. Boccini, S. Herold, *Biochemistry* **2004**, *43*, 16393–16404.
[44] I. Bytheway, M. B. Hall, *Chem. Rev.* **1994**, *94*, 639–658.
[45] C. J. Cramer, W. B. Tolman, *Acc. Chem. Res.* **2007**, *40*, 601–608.
[46] B. L. Westcott, J. H. Enemark, *Inorg. Electron. Struct. Spectrosc.* **1999**, *2*, 403–450.
[47] J. N. Armor, M. Buchbinder, *Inorg. Chem.* **1973**, *12*, 1086–1090.
[48] O. Pestovsky, A. Bakac, *J. Am. Chem. Soc.* **2002**, *124*, 1698–1703.
[49] M. H. Ford-Smith, N. Sutin, *J. Am. Chem. Soc.* **1961**, *83*, 1830–1834.
[50] C.-T. Lin, W. Bottcher, M. Chou, C. Creutz, N. Sutin, *J. Am. Chem. Soc.* **1976**, *98*, 6536–6544.
[51] A. Bakac, J. H. Espenson, *J. Am. Chem. Soc.* **1988**, *110*, 3453–3457.
[52] B. A. Barshop, R. F. Wrenn, C. Frieden, *Anal. Biochem.* **1983**, *130*, 134 –145.

Received: November 18, 2007
Published online: April 11, 2008

